# Solvent organization around the perfluoro group of coumarin 153 governs its photophysical properties: An experimental and simulation study of coumarin dyes in ethanol as well as fluorinated ethanol solvents

Saptarsi Mondal, Ritaban Halder, Biswajit Biswas, Biman Jana' , and Prashant Chandra Singh'

Citation: The Journal of Chemical Physics **144**, 184504 (2016); doi: 10.1063/1.4948704
View online: http://dx.doi.org/10.1063/1.4948704
View Table of Contents: http://aip.scitation.org/toc/jcp/144/18
Published by the American Institute of Physics

# Solvent organization around the perfluoro group of coumarin 153 governs its photophysical properties: An experimental and simulation study of coumarin dyes in ethanol as well as fluorinated ethanol solvents

Saptarsi Mondal,[1] Ritaban Halder,[2] Biswajit Biswas,[1] Biman Jana,[2,a)] and Prashant Chandra Singh[1,a)]
[1]*Department of Spectroscopy, Indian Association for the Cultivation of Science, Kolkata 700032, India*
[2]*Department of Physical Chemistry, Indian Association for the Cultivation of Science, Kolkata 700032, India*

(Received 28 December 2015; accepted 22 April 2016; published online 11 May 2016)

The self-aggregation property of the perfluoro group containing molecules makes it important in the research fields of biology and polymer and organic synthesis. In the quest of understanding the role of the perfluoro group on the photophysical properties of perfluoro-containing molecules in biologically important fluoroethanol solvents, we have applied photophysical as well as molecular dynamics simulation techniques to explore the properties of perfluoro groups containing molecule coumarin-153 (C153) in ethanol (ETH), monofluoroethanol (MFE), difluoroethanol (DFE), and trifluoroethanol (TFE) and compared them with the molecules without perfluoro moiety, namely coumarin-6H (C6H) and coumarin-480 (C480). In contrast to C6H and C480, the excited state lifetime of C153 in fluorinated ETHs is not monotonic. The excited state lifetime of C153 decreases in MFE and DFE as compared to ETH, whereas in TFE, it increases as compared to MFE and DFE. Molecular dynamics simulation reveals that the carbon terminal away from the OH group of fluorinated ETHs has a preferential orientation near the perfluoro ($CF_3$) group of C153. In MFE and DFE, the $CF_3$ group of C153 prefers to have a $CF_2$—F · · · H—(CHF) type of electrostatic interaction over $CF_2$—F · · · F—($CH_2$) kind of dispersion interaction which increases the rate of nonradiative decay, probably due to the electrostatic nature of the $CF_2$—F · · · H—(CHF) hydrogen bond. On the other hand, in TFE, C—F· · · F—C type of dispersion interaction, also known as fluorous interaction, takes place between the $CF_3$ groups of C153 and TFE which decreases the rate of nonradiative rate as compared to MFE and DFE, leading to the increased lifetime of C153 in TFE. Photophysical and MD simulation studies clearly depict that the structural organization of solvents and their interaction with the fluorocarbon group are crucial factors for the photophysical behavior of the fluorocarbon containing molecules. *Published by AIP Publishing.* [http://dx.doi.org/10.1063/1.4948704]

## I. INTRODUCTION

Fluorocarbons possess unusual but useful physicochemical properties. Molecules containing fluorocarbon group(s) have garnered significant interest because of its implication in the *de novo* designed proteins, fire retardants, anesthetics, and organic synthesis.[1–4] Several studies on the fluorinated analogues of hydrophobic amino acids have been performed in order to understand the role of fluorocarbon in the stability as well as biological activity of small proteins and peptides.[5–9] It has been found that fluorine substituted proteins stabilize their native structure in the guanidinium chloride, organic solvents, and urea more as compared to unsubstituted proteins without much affecting their biological activity.[5,7] Apart from this, fluorocarbon containing polymers have been reported as a unique material because of their very low coefficients of friction and outstanding chemical as well as thermal resistance properties.[10,11]

The C—F bond of fluorocarbons is stronger as well as longer compared to C—H. The electronegativity of the fluorine is higher which makes the C—F bond less polarazible as compared to C—H. A C—F bond is 14 kcal/mol more stable as compared to the C—H bond, and the dipole moment of the C—F bond is directionally opposite to C—H. The above discussed properties of C—F bond combinedly make perfluorinated molecules inert, extreme hydrophobic, and less polarazible which endue them with unusual phase segregating properties. There are few experimental reports in the literature where the self-aggregation capability of perfluoro group, also known as fluorous effect, has been predicted to stabilize small proteins and peptides.[1,3,5,8] All the informations have been obtained mainly through circular dichroism and the X-ray studies. Furthermore, theoretical and computational studies in the literature also corroborate the importance of fluorinated molecules towards the stability of proteins.[12–17] One of the most interesting observations is the enhance stability of proteins in the aqueous solution of trifluoroethanol (TFE) as compared to the bulk water.[16] The higher stability of the protein in the aqueous solution of TFE has been assigned to the self-aggregating property of TFE through the fluorous interaction.

The situation becomes more interesting when the solute and solvent both possess the perfluoro group. In this scenario, solvent molecules may arrange themselves to maximize the

a)Electronic addresses: pcbj@iacs.res.in and sppcs@iacs.res.in

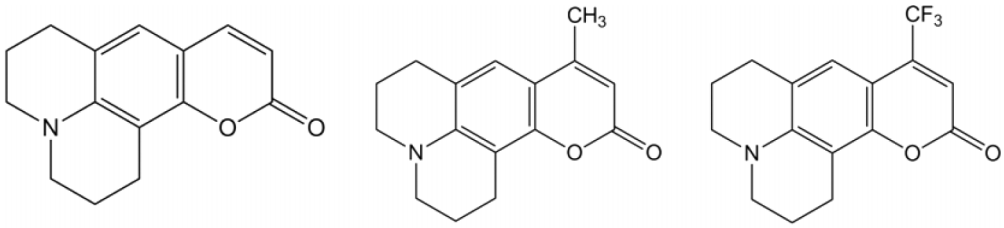


FIG. 1. Structure of C6H, C480, and C153 dyes.

fluorous effect within itself; hence, the interaction of the solute molecule with the solvent molecules will depend on the arrangement of the solvent molecules. In fact, several fluorinated amino acids and protein molecules have been synthesized and found to be more stable in fluorinated alcohols as compared to their nonfluorinated amino acids and protein analogs.[1,5,8] However, there is a dearth of molecular level information about the local environment and the nature of interactions between solvents and the perfluoro group of molecules, which is important to understand the enhanced stability of the fluorine containing molecules.

In order to get the answers of the above stated questions, we have used the photophysical as well as simulation techniques to study the properties of three different prototypical dyes coumarin-6H (C6H), coumarin-480 (C480), and coumarin-153 (C153) (structures are depicted in Figure 1) in ethanol (ETH), monofluoroethanol (MFE), difluoroethanol (DFE), and TFE solvents. It is well known that fluoro-ETHs especially TFE which induces the conformational transition of globular proteins and stabilizes predominantly the secondary structure of proteins. All three dyes have same skeleton except the presence of perfluoro group in C153 and $CH_3$ group in C480. We have taken three different fluorinated ethanol molecules to have a systematic understanding about the change of the solvent environment around the probe molecules on systematic fluorine substitution.

## II. METHODS

### A. Experimental set up and materials

Absorption spectra were measured with a Shimadzu 2401PC UV-vis spectrophotometer. Steady-state fluorescence emission spectra were recorded with a HORIBA Jobin Yvon Fluorolog 3 spectrometer. Fluorescence intensity decays were measured using time-correlated single-photon counting (TCSPC) setup of the IBH, Fluorocube. A picosecond diode laser of 408 nm (IBH nanoLEDs) was used as an excitation source. The emission was collected at the magic angle polarization and detected using a multiple channel photomultiplier (MCP, Hamamatsu, 5000U-09). The typical full width half maximum of the system was measured using a liquid scatterer and found to be ~40 ps. Fluorescence intensity decays were analyzed using IBH DAS6 software and were deconvoluted with the instrument response profile. Obtained data were fit with a single exponential $I(t) = \Sigma\ B \exp(-t/\tau)$, where $\tau$ is the fluorescence lifetime and B is the pre-exponential factor for that component of the decay. The quality of the fitting was judged by the calculation of the reduced chi-square ($\chi^2$) value and the distribution of the weighted residuals among the data channels. The obtained values of $\chi^2$ were close to 1 and the weighted residuals were randomly distributed around 0, indicating a high goodness of fit. The dye concentration of ~5 $\mu$M was used in this study. The quantum yield of all the dyes has been calculated using the standard method and the detail of the method has been provided in the supplementary material.[18,38]

ETH (99.9%), MFE (98%), DFE (97%), and TFE (99.5%) were purchased from Spectrochem (Mumbai, India), and distilled as well purged with $N_2$ before and during the measurements to make sure that there is no water content left in the solution. Laser grade dyes C480, C153, and C6H were purchased from Sigma Aldrich and were used as received. All measurements were carried out at ambient temperature (~25 °C).

### B. Molecular dynamics simulation

Molecular dynamics (MD) simulations of C153 and C6H in ETH, MFE, and TFE were carried out using the GROMACS molecular dynamics simulation package.[19] For each case, all atom and united atom simulations have been performed. The parameters for both C153 and C6H have been generated using automated topology builder software (ATB).[20] Both the all atom (OPLS-AA) and united atom (GROMOS 53a6) parameters for ETH were used as available in GROMACS topology. Similarly, the united atom parameters for TFE were used as available in the GROMOS 53a6 force field. We have modified the inbuilt all atom topology for TFE in OPLS-AA force field in order to reproduce the correct density of the system. We have constructed the topology of MFE by attaining the correct density of MFE via tuning its partial charges. In the present study, all the simulations began with the structure of C153 or C6H (dye) which was optimized by ATB followed by the solvation of dye molecule with ~2000 alcohol molecules. To generate a system with experimental concentration (~$\mu$M), one should take ~$10^6$ alcohol molecules per dye. However, for efficient computation, we choose to take ~2000 alcohols/dye as this number is enough to provide bulk-like solvation for the respective dye molecules. Each trajectory was equilibrated in a NPT ensemble for 10 ns at 300 K and 1 bar pressure for all the systems after steepest descent energy minimization of 5000 steps. Subsequently, the equilibrated configuration was subjected to a production run of another 50 ns in NPT

ensemble at 300 K and 1 bar pressure. The temperature was kept constant using the Nose-Hoover thermostat[21,22] with a time constant (τ) of 0.5 $ps^{-1}$ and the pressure of the system was kept constant by using the Parinello–Rahman barostat[23] with a τ of 1.0 $ps^{-1}$. Each simulation used a time-step of 2 fs with periodic boundary conditions. Non-bonded force calculation with a grid was employed for neighbor searching. Neighbor list generation was performed after every 10 steps. A cut-off radius of 1.2 nm was used for both neighbor list and van der Waal's interaction. To calculate the electrostatic interactions, we used PME[24] with a grid spacing of 0.16 nm and an interpolation order of four. Recently, the concept of sigma-hole has drawn significant interest to model the interactions involving halogen atoms.[25–28] However, it is important to note that halogen bonding interactions are important for molecules having either the chloride, bromide, or iodide groups and the effect of this interaction is found to be negligible for fluorine containing molecules.[29–32] Therefore, in our current study, we used simple force field for all the simulations without considering sigma-hole concept.

The excited state and ground state structure of C153 monomer and microhydrated in ETH, MFE as well as TFE has been calculated at the B3LYP/6-31G (d) using the Gaussian 09 Suite of program.[33]

## III. RESULTS AND DISCUSSION

Figure 2 represents the UV-vis as well as the steady-state emission spectrum of C6H, C480, and C153 in ETH, MFE, DFE, and TFE, respectively. The peak position of UV-vis as well as emission spectrum for these dyes in different solvents has been depicted in Table I. In general, UV-vis and emission spectra of all dyes in fluorinated ETHs are red shifted as compared to ETH. However, there is a noticeable difference in the emission spectrum for C153 in fluorinated ETHs as compared to C6H and C480. The emission spectrum for C153 in TFE is blue shifted as compared to MFE and DFE, in contrast to C6H and C480, where the emission spectrum gets monotonically red shifted from MFE to TFE. The trend of the emission spectrum in TFE indicates that the surroundings of C153 in TFE may be different as compared to C6H and C480.

To get more insight about the surrounding of these dyes in ETH and different fluorinated ETHs, we have measured the excited state lifetime (τ) of C6H, C480, and C153 in these solvents. Figure 3 shows the trace of the excited state decay along with the single exponential fitted plot of these traces corresponding to C6H, C480, and C153 in ETH, MFE, DFE, and TFE. The τ values for C6H, C480, and C153 in respective solvents are depicted in Table I. The τ value for C6H and C480 increases with the successive increase of fluorine on ETH which indicates that the excited state of C6H and C480 gets stabilized progressively by the successive addition of the fluorine on ETH. The other noticeable observation is that the value of τ for C6H is slightly less as compared to C480 in all these solvents. The excited state lifetime of probe in any solvents depends on the polarity of medium, excited state dipole moment of probe, and specific interaction between probe and solvent molecules. The observed trend of τ values for C6H and C480 in different solvents can be attributed to the solvent polarity. The $E_T(30)$ value has been used as a reliable way to express the polarity of solvents[34] and has been reported to be 51.9, 56.6, and 59.8 for ETH, MFE, and TFE respectively, indicating that the polarity of solvent increases with the successive fluorination of ETH, which causes the increased τ in different fluorinated ETHs. The slightly higher τ values of C480 as compared to C6H in different solvents have

TABLE I. The peak position of UV-vis (nm), steady state emission spectrum (nm), lifetime (ns), quantum yield ($\Phi_f$), radiative rate ($k_r$), and nonradiative rate ($k_{nr}$) in $s^{-1}$ for C6H, C480, and C153 in ETH, MFE, DFE, and TFE solvents.[a]

| System | UV-Vis (nm) | Emission (nm) | Lifetime (ns) | $\Phi_f$ | $k_r \times 10^8$ ($s^{-1}$) | $k_{nr} \times 10^8$ ($s^{-1}$) |
|---|---|---|---|---|---|---|
| | | | C6H | | | |
| ETH | 392 | 473 | 4.6 | 0.72 | 1.57 | 0.61 |
| MFE | 396 | 484 | 5.1 | 0.74 | 1.44 | 0.50 |
| DFE | 404 | 488 | 5.6 | 0.77 | 1.35 | 0.40 |
| TFE | 411 | 489 | 5.8 | 0.79 | 1.36 | 0.36 |
| | | | C480 | | | |
| ETH | 388 | 464 | 4.7 | 0.60 | 1.28 | 0.86 |
| MFE | 393 | 476 | 5.3 | 0.61 | 1.16 | 0.74 |
| DFE | 396 | 482 | 5.9 | 0.62 | 1.05 | 0.64 |
| TFE | 403 | 483 | 6.1 | 0.64 | 1.06 | 0.59 |
| | | | C153 | | | |
| ETH | 422 | 525 | 4.8 | 0.38 | 0.80 | 1.30 |
| MFE | 427 | 536 | 3.8 | 0.21 | 0.53 | 2.00 |
| DFE | 431 | 537 | 3.7 | 0.22 | 0.58 | 2.07 |
| TFE | 437 | 533 | 4.2 | 0.30 | 0.73 | 1.70 |

[a] ±0.05 ns is the maximum uncertainty associated with the evaluation of lifetime value.

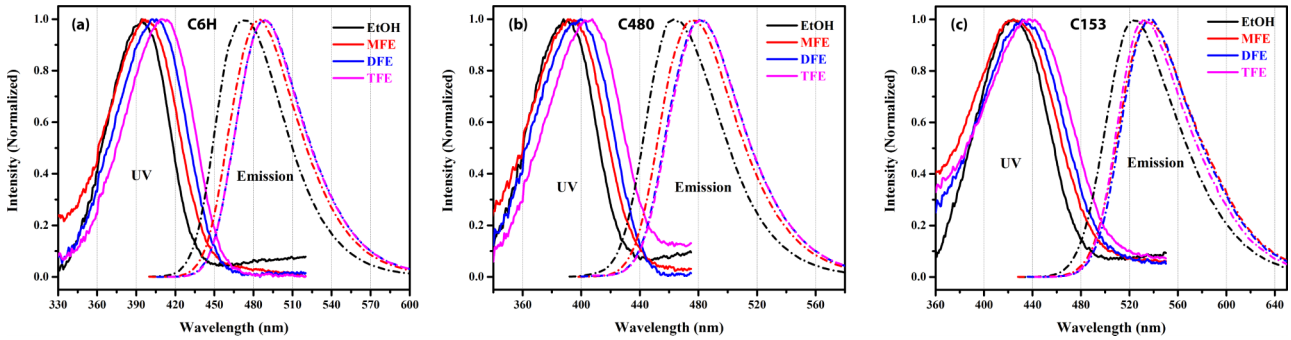


FIG. 2. UV-vis (solid line) and steady-state emission spectra (dotted line) of C6H, C480, and C153 in ETH, MFE, DFE, and TFE.

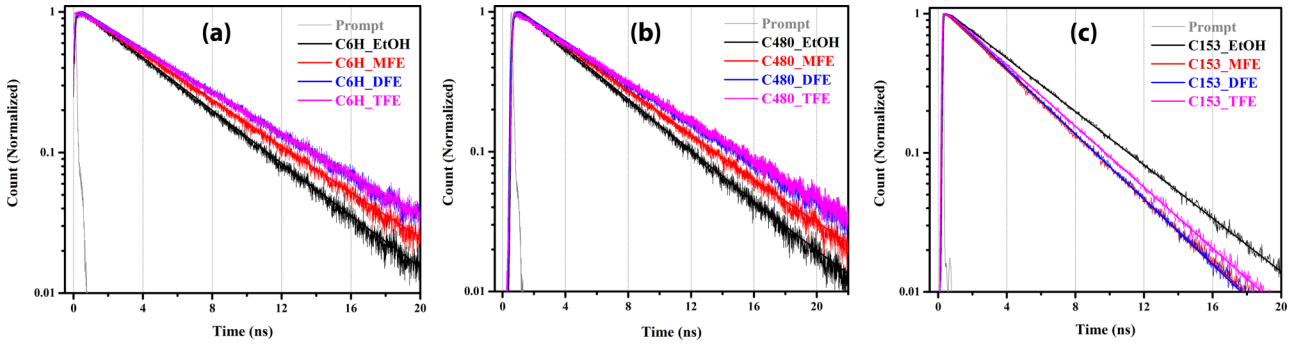


FIG. 3. Lifetime traces of C6H (a), C480 (b), and C153 (c) in ETH, MFE, DFE, and TFE.

been designated to the higher excited state dipole moment of C480 (13.1 D) as compared to C6H (9.3 D).[35,36]

The τ of C153 in ETH, MFE, DFE, and TFE has been found to be 4.8, 3.8, 3.7, and 4.2 ns respectively.[37] Interestingly, the τ of C153 in ETH is slightly higher as compared to C6H and C480, whereas in fluorinated ETHs, the τ of C153 is less as compared to C6H and C480. The increased τ value of C153 in ETH as compared to C6H and C480 could be due to the higher excited state dipole moment of C153 (14.5 D) as compared to C480 (13.1 D) and C6H (9.3 D).[35] However, the obtained trend of τ for C153 in fluorinated ETHs indicates that the solvent polarity and dipole moment of C153 are not significant factors as the solvent polarity of fluorinated ETHs is higher as compared to ETH as well as the excited dipole moment of C153 is higher as compared to C6H and C480. The other notable observation is that the trend of τ values of C153 in fluorinated ETHs is not monotonous like C6H and C480. The τ value of C153 in TFE is higher as compared to MFE and DFE which indicates that TFE interacts differently with C153 as compared to MFE and DFE. In summary, the observed lifetime of C153 in fluorinated ETHs indicates that the solvent environment near to C153 changes significantly with the fluorination of ETH.

C6H, C480, and C153 have same structure except the presence of different substituted groups as shown in Figure 1. The different trend of τ values of C153 as compared to C6H and C480 in different fluorinated ETHs indicates that the $CF_3$ group of C153 plays a significant role in its photophysical behavior in different fluorinated ETHs. The $CF_3$ group of C153 can specifically interact with fluorinated ETHs in different senses which can cause the change in radiative and nonradiative decay rates of C153 differently as compared to other dyes in fluorinated ETHs,

$$\Phi_F = \frac{k_r}{k_r + k_{nr}}, \quad (1)$$

$$\tau = \frac{1}{k_r + k_{nr}}. \quad (2)$$

To further shed the light on different behaviors of C153 in fluoroETHs, we have calculated the quantum yield (ϕ), radiative ($k_r$), and nonradiative rate ($k_{nr}$) of different dyes in ETH as well as fluorinated ETHs, and the values are given in Table I. The ϕ values of different dyes in ETH and fluorinated ETHs have been calculated by the standard method,[18] whereas rate of $k_r$ and $k_{nr}$ processes has been calculated using Equations (1) and (2). It can be seen that the value of $k_r$ as well as $k_{nr}$ decreases with the successive fluorination of ETH for C6H and C480. The value of $k_r$ for C153 in MFE and DFE decreases as compared to ETH which is similar to the case of C6H and C480; however, the value of $k_{nr}$ for C153 in MFE and DFE increases as compared to ETH case, opposite to the behavior of C6H and C480. The increase in the value of $k_{nr}$ of C153 in MFE as well as DFE is higher as compared to the decrease in $k_r$. Interestingly, the value of $k_r$ of C153 in TFE is slightly higher, whereas the value of $k_{nr}$ is less as compared to MFE and DFE. However, the amount of decrease in the value of $k_{nr}$ is more as compared to the increase of $k_r$ for C153 in TFE. The calculation of photophysical parameters indicates that nonradiative processes are mainly involved behind the different τ values of C153 in fluoro-ETHs; however, it does not provide any information about the environments such as hydrogen bonding which cause a decrease or increase in the nonradiative rate.

In order to understand the environment around dyes in ETH and fluorinated ETHs, we have performed MD simulation for C6H and C153 in ETH, MFE, and TFE. C480 shows the same behavior as C6H; hence, C6H has been chosen. We have looked into the solvent organization around C═O moiety, oxygen moiety of ester group, and nitrogen atom of both the dyes to investigate the indirect effect of the $CF_3$ group (for C153) on hydrogen bonding with solvents around these moieties. We have also explored the solvent organization around $CF_3$ moiety of C153 to investigate the possibility of the formation of specific solute-solvent interactions.

To explore the structural organizations of solvent molecules around the oxygen atom of C═O moiety in C6H, we have calculated radial distribution function of different atoms of solvent around it. Figure 4(a) shows the radial distribution function (g(r)) of oxygen atom of alcohols (denoted as $O_1$) from the oxygen atom of C═O group of C6H. The height of the first peak is higher for the TFE as compared to ETH which indicates the higher probability of hydrogen bonding interaction between the C═O of C6H and H—$O_1$ of alcohols (C═O···H—$O_1$) which is because of the higher acidity of TFE as compared to ETH. Surprisingly, the height of the first peak of MFE is less as compared to ETH inferring a comparatively lower probability of C═O···H—$O_1$ hydrogen bonding interactions for MFE. Decreased intensity of the first peak in the case of MFE is counterintuitive as the acidity of MFE is higher compared to ETH. Hence, we

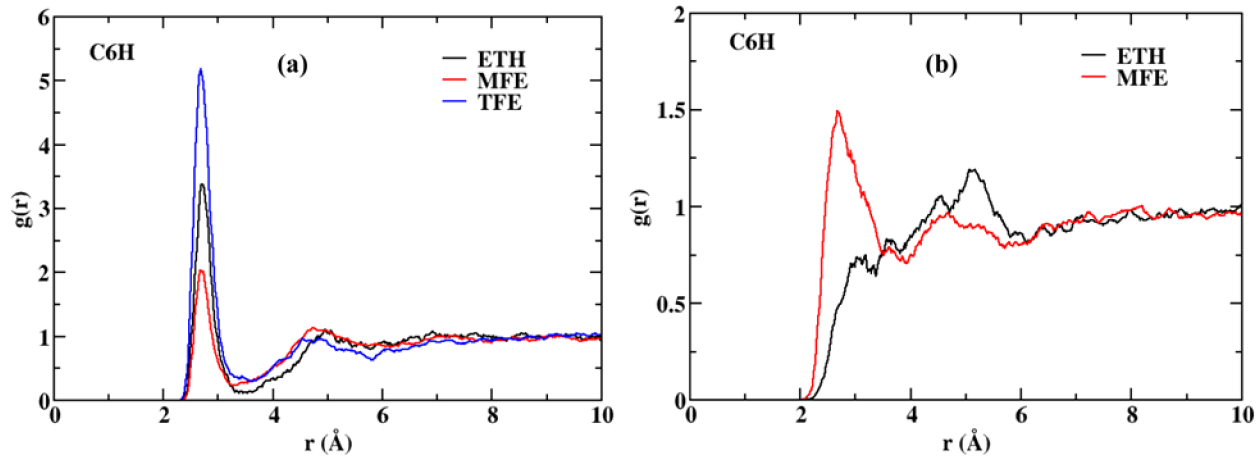


FIG. 4. Structural organization of solvent molecules near C=O moiety of C6H. (a) Radial distribution function of $O_1$ atom of alcohols from the C=O moiety of C6H. The peak height of the first peak indicates the probability of the formation of C=O···H—$O_1$ interaction. (b) Radial distribution function of hydrogen atoms attached to $C_3$ atom of ETH and TFE from C=O moiety of C6H. Note that the distinct feature of the first peak of MFE indicating the formation of specific C=O···H—C interactions.

have calculated the radial distribution function of hydrogen atoms attached to terminal carbon atoms (away from OH and denoted as $C_3$, Figure S1[38]) of ETH and MFE around the C=O moiety of C6H in order to probe the possibility of the C=O···H—C interaction; the results are shown in Figure 4(b). We indeed find a dramatic increase in the first peak of MFE as compared to ETH indicating the possibility of formation of C=O···H—C interaction in MFE. The higher probability of hydrogen bonding between the C—H group of MFE and C=O moiety of C6H is also supported by the fact that fluorine substitution makes the C—H group of MFE more acidic as compared to ETH. Therefore, the decrease in the first peak of the radial distribution function for the oxygen atoms of MFE (Figure 4(a), red line) is due to the competition between the C=O···H—$O_1$ and C=O···H—C types of interactions in C6H. Further, we have investigated the solvent organizations around the C=O moiety of C153 in order to probe the possibility of disruption of hydrogen bonding due to the $CF_3$ group of C153 as compared to C6H. The radial distribution functions for C153 (Figure S2[38]) in all three solvents are very similar to the C6H, indicating that the solvent environment near C=O moiety does not get affected by the $CF_3$ substitution.

Next, we have explored the structural organizations of alcohols around nitrogen atom as well as oxygen atom of ester group of both dyes (C6H and C153), as both the groups of dyes are potential hydrogen bonding sites. The results presented in the supplementary material (Figures S3 and S4[38]) clearly show that the structural organizations around these two moieties are very similar for both the dyes, suggesting that indirect effect of $CF_3$ group on the surrounding environment near dyes is not significant.

The hydrogen bonding network around the C=O moiety as well as other two moieties (nitrogen and oxygen of ester) of C6H and C153 is the same; hence, we have investigated the solvent environment around the $CF_3$ group of C153 in these three alcohols. We have calculated the radial distribution function of $C_3$ and $O_1$ atoms of alcohols from the F atoms of the $CF_3$ moiety of C153 to explore the possibility of preferential interaction. Figure 5(a) shows the g(r) for the $C_3$ (red line) as well as $O_1$ (black line) of TFE with respect to the F atoms of the $CF_3$ moiety of C153. We find a clear signature of the preferential interaction of $CF_3$ moiety of C153 by the $C_3$ end of TFE (blue circle, Figure 5(a)). We have calculated the similar distribution for other two alcohols and found the similar types of preferential solvation by $C_3$

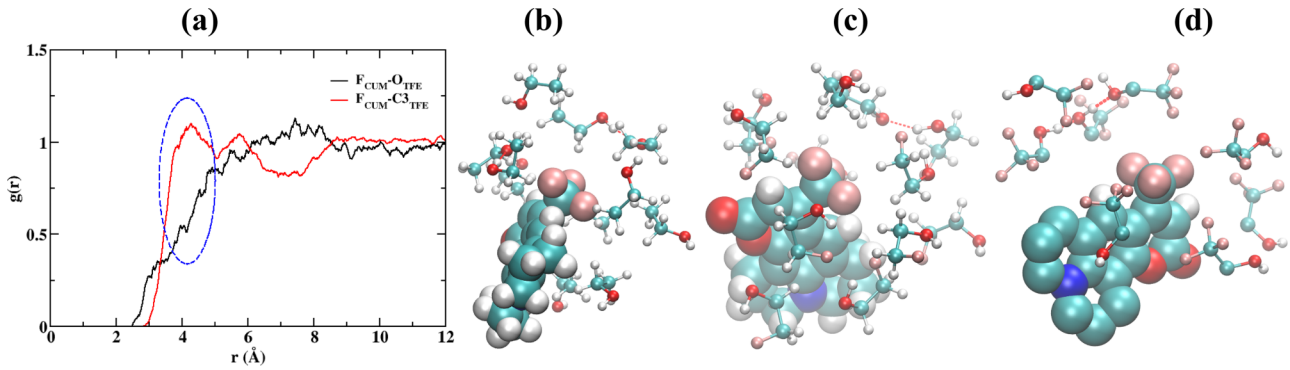


FIG. 5. Solvent organizations around $CF_3$ moiety of C153. (a) Radial distribution functions of $O_1$ and $C_3$ atoms of TFE from the $CF_3$ moiety of C153. Note the comparatively enhanced first peak value for $C_3$ atoms indicating a preferential solvation by $C_3$ end of TFE. Similar preferential solvation by other alcohols is also seen (supplementary material, Fig. S5[38]). Pictorial representation of the first solvation layer around $CF_3$ moiety of C153 in (b) ETH, (c) MFE, and (d) TFE. Note the preferential solvation by $C_3$ end of alcohols in all the cases.

end as compared to $O_1$ end of alcohols as presented in the supplementary material (Figure S5[38]). We have presented a pictorial representation of the solvent organization around the $CF_3$ group of C153 in these three alcohols in Figures 5(b)-5(d) which clearly depict that $CH_3$ group of ETH, $CH_2F$ group of MFE, and $CF_3$ group of TFE are organized closely to the $CF_3$ group of C153. It is interesting to mention here that the hydrogen bonding between the alcohols around the $CF_3$ moiety of C153 is different from the C═O moiety of C153. Around the C═O moiety of C153, the O—H···O hydrogen bonding between the solvent molecules is reorganized due to the interaction of O—H group of solvent with the C═O moiety of C153. In contrast to it, O—H···O interaction between the solvent molecules is preserved around the $CF_3$ terminal of C153 in order to maximize the preferential interaction of $CF_3$ moiety of C153 by the $C_3$ end of solvent molecule. In finite temperature molecular dynamics simulations, the stabilization through the formation of hydrogen bond (O···H—O) network among alcohols in the bulk dominates over the stabilization of $CF_3$ (C153)···HO (ETH/MFE/TFE) interactions.

Finally, we have investigated about the presence of specific interactions between the $CF_3$ group of C153 and the $C_3$ end of the alcohols. In Figure 6, we have shown the specific atoms present within 3.5 Å of the fluorine of $CF_3$ (C153) in ETH, MFE, and TFE. In ETH case, the hydrogen attached to the C3 of ETH has been found to be near to the $CF_3$ of C153. For MFE, the situation is a bit different as it has both CF and $CH_2$ environments in the $CH_2F$ group which can interact with the $CF_3$ moiety of C153. We have found that more number (~8) of hydrogen atoms as compared to the fluorine attached with the C3 of MFE prefers to interact with the $CF_3$ group of MFE as shown in Figure 6(a). To explore details of the solvent organization, we have calculated the radial distribution function for hydrogen as well as fluorine of $CH_2F$ moiety of MFE with respect to the fluorine of $CF_3$ (C153). We have observed a shift in the first peak of radial distribution function for hydrogen (red line, Figure 6(a)) as compared to fluorine (black line, Figure 6), indicating that the hydrogen of $CH_2F$ group prefer to interact with the $CF_3$ group of C153 through $CF_2$ e F (C153)···H—CHF (MFE) type of interactions (Figure 6(b)). The electrostatic attraction between fluorine of $CF_3$ (C153) and hydrogen of $CH_2F$ (MFE) dominates over the dispersion interactions between the fluorine of $CF_3$ (C153) and CF (MFE). The electrostatic attraction gets stabilized due to the fact that the partial charge on the hydrogen of $CH_2F$ moiety is considerably higher (+1.20e) as compared to ETH (+0.60e) due to the electron withdrawing nature of fluorine. From the case of MFE, one can intuit the presence of comparatively stronger interaction between the $CF_3$ (C153) and H—$CF_2$ (DFE) for DFE. Similar to MFE, hydrogen attached with the $C_3$ group of ETH gets closer to the CF3 of C153; however, there is very weak electrostatic interaction takes place between them due to the absence of any electron withdrawing atoms on $CH_3$ of ETH. In the case of TFE, it can be clearly seen that the fluorine of TFE prefers to come closer to the fluorine of C153 (Figure 6(c)) and fluorous interaction (F···F) between the CF3 group of C153 and CF3 group of TFE takes place. Unlike to the case of MFE, the dispersion interaction between the $CF_3$ of C153 and $CF_3$ of TFE dominates over the electrostatic repulsion.

In order to find the change in the structure of C153 in different alcohols at the ground ($S_0$) and excited ($S_1$) states, we have optimized the microhydrated structures of C153 obtained from MD simulations in ETH, MFE, and TFE using the polarized continuum model (PCM) at the B3LYP/6-31G (d) level of theory in the $S_0$ as well as $S_1$ states. The structures and geometrical parameters obtained from calculations are shown in the supplementary material (Figures S6 and S7, Tables S1 and S2[38]). We could not find any noticeable change in the structure of dye in the $S_1$ state as compared to the $S_0$ state except the shortening of intermolecular hydrogen bonding distance between the binding site of C153 and alcohol, which indicates that the structure obtained around the $CF_3$ group of C153 in different fluorinated alcohols from the MD simulation will be more strengthened in the $S_1$ state as compared to the $S_o$ state.

It is worthwhile to mention here that the equilibrium structures around dye molecules discussed above must have

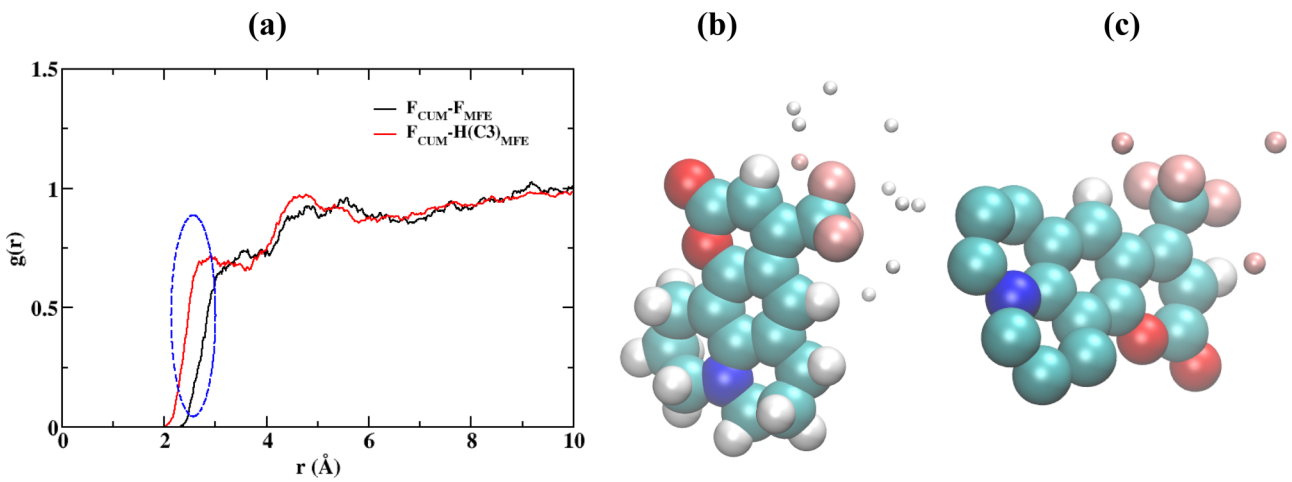


FIG. 6. Specific interactions of $CF_3$ moiety of C153 with MFE. (a) Radial distribution functions of F and H ($C_3$) atoms of MFE from $CF_3$ moiety of C153. Shifting of the first peak towards lower distances for H ($C_3$) atoms compared to F atoms indicates the possibility of the formation of specific $CF_2$—F (C153)···H—CHF (MFE) interactions. Pictorial representations of the atoms present within 3.5 Å from the $CF_3$ moiety of C153 in (b) MFE and (c) TFE. Note the presence of mostly H ($C_3$) atoms near to $CF_3$ in MFE.

a timescale for reorganizations. This timescale, commonly known as solvation time scale, is generally very fast and the corresponding time correlation functions decays within few hundreds of picoseconds at most, which is significantly smaller than lifetime of the excited state of the dye. Hence, surrounding equilibrium solvent organizations (that will change the local dielectric constant and also the specific interactions) determine the lifetime of the dye molecules. We have also explored the solvent organization around dye in its excited state and compared them with the ground state (Figure S8[38]). The structural organization in both the states is found to be quite similar to each other and similar to the quantum chemical calculations.

The MD simulations clearly depict that the $CF_3$ group of C153 is the main difference in creating the different organizations of fluoroETHs as compared to the C6H. The $CF_3$ group of C153 interacts with fluoroETHs in different passion. Experimental and simulation studies together suggest that the electrostatic interaction between the C—H group of MFE and DFE with $CF_3$ group of C153 increases the rate of nonradiative decay which decreases the τ values of C153 in MFE and DFE, whereas the fluorous interaction takes place between $CF_3$ groups of C153 and TFE due to which the rate of nonradiative rate decreases as compared to MFE and DFE; hence, τ values of C153 in TFE is higher as compared to MFE and DFE.

## IV. CONCLUSION

Steady state emission spectrum of all the dyes in fluorinated ETHs is red shifted as compared to ETH. However, there is a noticeable difference in the emission spectrum for C153 in fluorinated ETHs as compared to C6H and C480. In contrast to C6H and C480, the emission spectrum for C153 in TFE is blue shifted as compared to MFE and DFE, indicating that the surroundings of C153 in TFE may differ as compared to C6H and C480. The τ of C6H and C480 increases with the successive increase of fluorine on the ETH which is in line with the polarity of the solvent molecules. However, the τ value of C153 is not monotonic in fluorinated ETHs and its values in MFE and DFE are less as compared to ETH, whereas increased in TFE as compared to MFE and DFE. MD simulation shows that the structural organizations of alcohols around C═O groups of both C6H and C153 are similar, indicating that the $CF_3$ of coumarin plays an important role in the different τ value of C153 in fluorinated ETHs. It has been found that the carbon terminal away from the OH group of fluorinated ETHs has a preferential orientation near the $CF_3$ group of C153. In MFE and DFE, the $CF_3$ group of C153 prefers to have a $CF_2$—F···H—(CHF) type of electrostatic interactions over $CF_2$—F···F—($CH_2$) kind of dispersion interactions. This specific $CF_2$—F···H—(CHF) type of electrostatic interaction probably opens up a non radiative decay channel in the excited state of C153. On the other hand, in TFE solvent, C—F···F—C type of dispersion interaction, also known as fluorous interaction, takes place between the $CF_3$ groups of C153 and TFE which decreases the rate of nonradiative decay, resulting in the higher lifetime of C153 in TFE as compared to MFE and DFE. This study describes the role of the perfluoro group on the photophysical properties of perfluoro containing molecule in different fluorinated ETHs which may be useful in understanding the role of the perfluoro group in the conformational dynamics as well as enhanced stability of fluorinated protein in various fluorinated ETH solvents.

## ACKNOWLEDGMENTS

This work is supported by the research grant provided by the Council of Scientific and Industrial Research [Grant No. 01(2803)/14/EMR-II], and Department of Science and Technology [Grant No. EMR/2015/001605] India. We thank the CRAY supercomputing facility at IACS for computational support. B.B. and R.H. thank CSIR for the fellowship.

[1]B. C. Buer, R. de la Salud-Bea, H. M. Al Hashimi, and E. N. G. Marsh, Biochemistry **48**, 10810 (2009).
[2]W.-Q. Deng, V. Molinero, and W. A. Goddard, J. Am. Chem. Soc. **126**, 15644 (2004).
[3]E. N. G. Marsh, Acc. Chem. Res. **47**, 2878 (2014).
[4]P. Zhou, J. Zou, F. Tian, and Z. Shang, J. Chem. Inf. Model. **49**, 2344 (2009).
[5]B. C. Buer, B. J. Levin, and E. N. G. Marsh, J. Am. Chem. Soc. **134**, 13027 (2012).
[6]B. C. Buer and E. N. G. Marsh, Protein Sci. **21**, 453 (2012).
[7]B. C. Buer, J. L. Meagher, J. A. Stuckey, and E. N. G. Marsh, Proc. Natl. Acad. Sci. U. S. A. **109**, 4810 (2012).
[8]H.-P. Chiu, B. Kokona, R. Fairman, and R. P. Cheng, J. Am. Chem. Soc. **131**, 13192 (2009).
[9]H.-Y. Lee, K.-H. Lee, H. M. Al-Hashimi, and E. N. G. Marsh, J. Am. Chem. Soc. **128**, 337 (2006).
[10]B. Ameduri and B. Boutevin, J. Fluorine Chem. **2005**, 221–229 (2005).
[11]K. Matsumoto, M. Kubota, H. Matsuoka, and H. Yamaoka, Macromolecules **32**, 7122–7127 (1999).
[12]K. Gast, D. Zirwer, M. Müller-Frohne, and G. Damaschun, Protein Sci. **8**, 625 (1999).
[13]J. T. Gerig, J. Phys. Chem. B **119**, 5163 (2015).
[14]M. Guo and Y. Mei, J. Mol. Model. **19**, 3931 (2013).
[15]S. Jalili and P. Amani, J. Mol. Liq. **197**, 27 (2014).
[16]D. Roccatano, G. Colombo, M. Fioroni, and A. E. Mark, Proc. Natl. Acad. Sci. U. S. A. **99**, 12179 (2002).
[17]M. D. Schuh and M. C. Baldwin, J. Phys. Chem. B **110**, 10903 (2006).
[18]G. Jones, W. R. Jackson, C. Y. Choi, and W. R. Bergmark, J. Phys. Chem. **89**, 294 (1985).
[19]D. van der Spoel, E. Lindahl, B. Hess, A. R. van Buuren, E. Apol, P. J. Meulenhoff, D. P. Tieleman, A. L. T. M. Sijbers, K. A. Feenstra, R. van Drunen, and H. J. C. Berendsen, Gromacs User Manual, 2014.
[20]S. Canzar, M. El-Kebir, R. Pool, K. Elbassioni, A. K. Malde, A. E. Mark, D. P. Geerke, L. Stougie, and G. W. Klau, J. Comput. Biol. **20**, 188 (2013).
[21]W. G. Hoover, Phys. Rev. A **31**, 1695 (1985).
[22]S. Nosé, J. Chem. Phys. **81**, 511 (1984).
[23]M. P. A. Rahman, J. Appl. Phys. **52**, 7182 (1981).
[24]D. Frenkel and B. Smit, *Understanding Molecular Simulation: From Algorithms to Applications*, 2nd ed. (Academic, San Diego, CA, 2002).
[25]W. L. Jorgensen and P. Schyman, J. Chem. Theory Comput. **8**, 3895 (2012).
[26]P.-A. Cazade, H. Tran, T. Bereau, A. K. Das, F. Kläsi, P. Hamm, and M. Meuwly, J. Chem. Phys. **142**, 212415 (2015).
[27]P. Politzer, J. S. Murray, and T. Clark, Phys. Chem. Chem. Phys. **15**, 11178 (2013).
[28]P. Politzer, J. S. Murray, and T. Clark, Phys. Chem. Chem. Phys. **12**, 7748 (2010).
[29]P. Politzer, P. Lane, M. C. Concha, Y. Ma, and J. S. Murray, J. Mol. Model. **13**, 305 (2006).
[30]P. Politzer, J. S. Murray, and M. C. Concha, J. Mol. Model. **13**, 643 (2007).
[31]K. Eskandari and M. Lesani, Chem. - Eur. J. **21**, 4739 (2015).
[32]K. Eskandari and H. Zariny, Chem. Phys. Lett. **492**, 9 (2010).
[33]M. J. Frisch, G. W. Trucks, H. B. Schlegel, G. E. Scuseria, M. A. Robb, J. R. Cheeseman, G. Scalmani, V. Barone, B. Mennucci, G. A. Petersson *et al.*, GAUSSIAN 09, Revision B.01, Gaussian, Inc., Wallingford, CT, 2010.
[34]C. Reichardt, Chem. Rev. **94**, 2319 (1994).

[35]R. J. Cave and E. W. Castner, J. Phys. Chem. A **106**, 12117 (2002).
[36]D. Hessz, B. Hégely, M. Kállay, T. Vidóczy, and M. Kubinyi, J. Phys. Chem. A **118**, 5238 (2014).
[37]M. L. Horng, J. A. Gardecki, A. Papazyan, and M. Maroncelli, J. Phys. Chem. **99**, 17311 (1995).
[38]See supplementary material at http://dx.doi.org/10.1063/1.4948704 for the method of quantum yield measurement, the radial distribution data to show the structural organization of solvent molecules near C═O moiety of C153 as well as the structural organization of $O_1$ and $C_3$ atoms of ETH and MFE from the $CF_3$ moiety of C153, and radial distribution functions of $O_1$ of alcohols around the nitrogen atom as well as oxygen of the ester group of C153 and C6H in ETH, MFE, and TFE. Quantum chemical calculation results and their description about the microhydrated structure of C153 in different fluorinated ETHs at the ground and excited states.